Small-Molecule Activation

DOI: 10.1002/anie.201003001

Spontaneous Dihydrogen Activation by Neutral TaO_4 Complex at Cryogenic Temperatures**

Mingfei Zhou, Caixia Wang, Zhen hua Li, Jia Zhuang, Yanying Zhao, Xuming Zheng, and Kangnian Fan*

Catalytic hydrogenation is one of the most important reactions in industry.[1] The activation of dihydrogen by metal centers is a fundamental step in nearly all metal catalytic hydrogenation reactions.[2] Great efforts have been made to split the H–H bond at metal centers under mild conditions.[3–8] Traditional homogeneous hydrogenation catalysts are based on precious metals, on which dihydrogen splitting often proceeds by hemolytic cleavage to form metal hydride complexes, which can then transfer hydrogen atoms to organic or other substrates.[9] A second mechanism, heterolytic cleavage of dihydrogen into a hydridic and protic functionality, has also been observed for many transition-metal complexes.[10]

Transition-metal oxides are vital heterogeneous catalysts or supports in many processes involving H_2. Considerable theoretical investigations have been focused on H_2 adsorption and heterolytic dissociation on metal oxide surfaces.[2,11] The reactions of bare transition-metal oxide cations with dihydrogen have been studied in the gas phase with mass spectrometric techniques to provide useful insight into the elementary steps of catalytic reactions and to characterize reactive intermediates that have previously not been within reach of condensed-phase techniques.[12–14] In contrast to cationic reaction systems, neutral transition-metal oxide reactions have gained much less attention, in part because of the experimental challenges faced in detecting neutral species in the gas phase.[15] Herein we report a joint matrix-isolation infrared spectroscopic and theoretical study of dihydrogen activation by neutral tantalum oxide molecules. We found that, upon annealing, the ground-state TaO_4 d^0 complex reacts spontaneously with dihydrogen to form $[HTaO(OH)(\eta^2\text{-}O_2)]$, which involves both the hydridic (H^-) and the protic (H^+) functionalities.

We studied the reactivity of tantalum oxides in different oxidation states (TaO (II), TaO_2 (IV) and TaO_4 (V)) by matrix-isolation infrared absorption spectroscopy, which has previously been described in detail.[16] The tantalum oxide reactants were prepared either by pulsed laser evaporation of bulk Ta_2O_5 target or by the reactions of laser-evaporated tantalum atoms with dioxygen in solid argon. As has been reported previously,[17] pulsed laser evaporation of bulk Ta_2O_5 target under controlled laser energy followed by condensation with pure argon formed only the TaO and TaO_2 molecules.[18] Figure 1 shows the spectra in a selected region

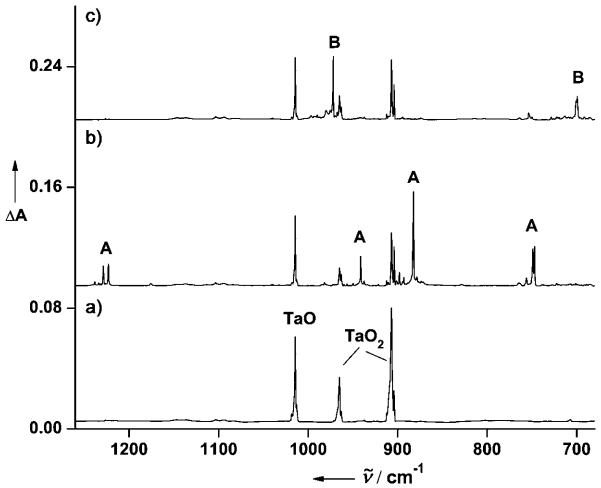

Figure 1. Infrared spectra in 1260–650 cm^{-1} region from co-deposition of laser-evaporated tantalum oxides with 2.0% H_2 in argon: a) 1 h of sample deposition at 4 K, b) after 25 K annealing, and c) after 20 min of visible-light irradiation ($400 < \lambda < 580$ nm).

from co-deposition of laser-evaporated tantalum oxides with a H_2/Ar sample (2.0% H_2 molar ratio). The spectra in other regions are shown in Figure S1 in the Supporting Information. Besides the TaO and TaO_2 absorptions, two groups of new absorptions were produced (labeled as A and B in Figure 1). The group A absorptions were produced on annealing at the expense of the TaO_2 absorptions. When the sample was subjected to broad-band irradiation using the high-pressure mercury arc lamp with a 400 nm long-wavelength pass filter ($400 < \lambda < 580$ nm), the group A absorptions were destroyed, whereas the group B absorptions were produced. The experiment was repeated using the bulk Ta_2O_5 target and the mixed H_2/O_2/Ar sample (2.0% H_2 + 0.1% O_2) as reagent gas, and the resulting spectra are shown in Figure 2 and Figure S2 in

[*] Prof. Dr. M. F. Zhou, Prof. Dr. Z. H. Li, J. Zhuang, Prof. Dr. K. N. Fan
Department of Chemistry
Shanghai Key Laboratory of Molecular Catalysts and Innovative Materials
Advanced Materials Laboratory, Fudan University
Shanghai 200433 (China)
Fax: (+86) 21-6564-3532
E-mail: mfzhou@fudan.edu.cn
C. X. Wang, Dr. Y. Y. Zhao, Prof. Dr. X. M. Zheng
Department of Chemistry, Zhejiang Sci-Tech University
Hanzhou (China)

[**] This work was supported by NKBRSF (2007CB815203, 2009CB623506 and 2010CB732306) and NSFC (20773030).

Supporting information for this article is available on the WWW under http://dx.doi.org/10.1002/anie.201003001.

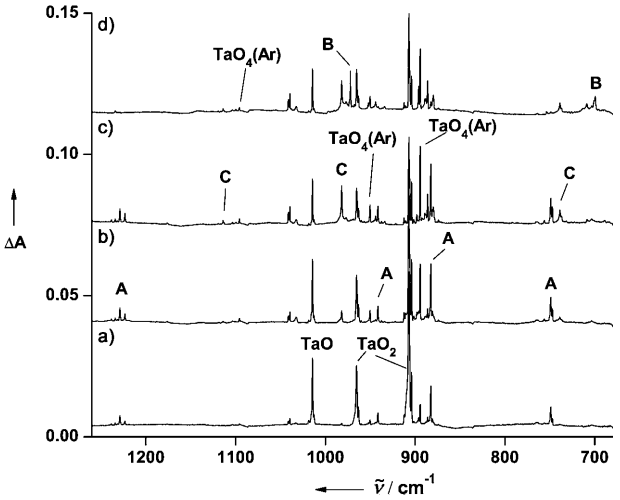

Figure 2. Infrared spectra in 1260–680 cm^{-1} region from co-deposition of laser-evaporated tantalum oxides with 0.1 %O_2 + 2.0 % H_2 in argon: a) 1 h of sample deposition at 4 K, b) after 22 K annealing, c) after 25 K annealing, and d) after 20 min of visible light irradiation ($400 < \lambda < 580$ nm).

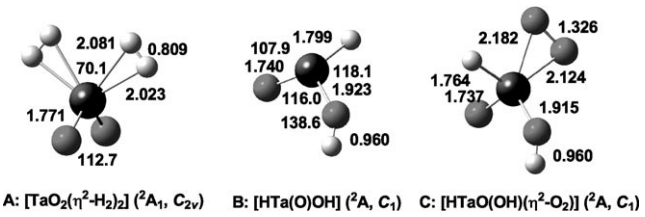

Figure 3. Optimized structures (bond lengths in angstroms, bond angles in degrees) of the species involved in the TaO_2 + H_2 and TaO_4 + H_2 reactions.

the Supporting Information. In this experiment, the TaO_2 molecule interacts readily with dioxygen on annealing to form the side-on bonded tantalum dioxide–dioxygen complex, TaO_4, which is trapped in solid argon as a TaO_4(Ar) complex.[19] Besides the group A and B absorptions, a third group of absorptions (labeled as C) appeared on low-temperature annealing, markedly increased upon high-temperature annealing, and slightly decreased upon irradiation with visible light. Note that the group C absorptions were not observed in the experiment without O_2 doping (Figure 1). Experiments were also performed using a tantalum metal target. The spectra from codeposition of laser-evaporated tantalum atoms with the mixed H_2/O_2/Ar sample (0.05 %O_2 + 2.0 % H_2 molar ratios) show that the ground state tantalum atoms react with dioxygen to give the inserted tantalum dioxide molecules, which further react with additional dioxygen to form TaO_4. The group A, B, and C absorptions were also formed on annealing or photolysis (see Figures S3 and S4 in the Supporting Information). Isotopic substitutions (HD, D_2, and $^{18}O_2$) were employed for product identification based on isotopic shifts and absorption splitting. The spectra are shown in Figures S5–S9 in the Supporting Information.

The group A absorptions are assigned to different vibrational modes of the $TaO_2(\eta^2\text{-}H_2)_2$ complex (Table S2 in the Supporting Information). The 882.6 and 941.4 cm^{-1} absorptions are due to the antisymmetric and symmetric OTaO stretching modes, which are about 24.4 and 23.9 cm^{-1} red-shifted from the corresponding absorptions of TaO_2 in solid argon. Quantum chemical calculations were performed to validate the experimental assignment.[20] The $[TaO_2(\eta^2\text{-}H_2)_2]$ complex was predicted to have an $^2A_1$ ground state with C_{2v} symmetry (Figure 3), which can be viewed as being formed by the interaction of ground-state TaO_2 ($^2A_1$) and $2H_2$. Similar to the previously characterized metal dihydrogen complexes,[2,21,22] the H_2 subunits are side-on bonded to the tantalum metal center and lie in the same plane, that is perpendicular to the OTaO plane. The $^2A_1$ ground-state TaO_2 molecule has an electron configuration of (core) $(a_1)^1(b_1)^0$. The highest singly occupied (SOMO) a_1 orbital is primarily a hybrid of the Ta 6s and 5d orbitals that is polarized away from the O atoms. As a result of σ repulsion, the H_2 molecule in $[TaO_2(\eta^2\text{-}H_2)]$ binds very weakly to the TaO_2 moiety with very long Ta–H bonds and a binding energy of nearly zero. No absorption bands due to the $TaO_2(\eta^2\text{-}H_2)$ complex were observed in the experiments. Molecular orbital and natural bond orbital (NBO) analysis showed that the SOMO of $[TaO_2(\eta^2\text{-}H_2)_2]$ is a bonding orbital between the σ_{H-H}* orbitals of the two H_2 units, and the 5d orbital of Ta and the two σ_{H-H}* orbitals have significant overlap with each other (see Figure S10 in the Supporting Information). The overlap between the two σ_{H-H}* orbitals enhances the interaction between the H_2 units and the TaO_2 moiety in $[TaO_2(\eta^2\text{-}H_2)_2]$.

Absorber B was produced under irradiation with visible light ($400 < \lambda$ 580 nm) at the expense of the group A absorptions, suggesting that the absorber of group B absorptions is due to a structural isomer or photoproduct of species A. The spectral features indicate that the 3715.0, 1780.5, 972.1, and 701.1 cm^{-1} absorptions are due to O-H, Ta-H, Ta=O, and Ta-OH stretching vibrations (Table S3 in the Supporting Information). Therefore, species B should be due to [HTaO(OH)] or $[HTaO(OH)(\eta^2\text{-}H_2)]$. Since no obvious H–H stretching absorption was observed, the group B absorptions are attributed to the [HTaO(OH)] molecule, which was predicted to have a doublet ground state without symmetry (Figure 3).

Ten absorption bands were observed for absorber C (Table 1). The 981.8 cm^{-1} absorption is due to a terminal Ta=O stretching vibration. The spectral features indicate that the much weaker 1113.8 cm^{-1} absorption is due to an O–O stretching vibration with two slightly inequivalent O atoms. The same mode of TaO_4(Ar) is observed at 1095.7 cm^{-1} in solid argon.[18,19] The 1838.7 cm^{-1} absorption is due to a Ta–H stretching vibration. The band position and isotopic frequency shifts imply that the 3699.3 cm^{-1} absorption originates from an O–H stretching vibration. The 739.0 cm^{-1} absorption is the corresponding Ta–OH stretching vibration. The above discussions led us to propose the assignment of the group C absorptions to different vibrational modes of the $[HTaO(OH)(\eta^2\text{-}O_2)]$ complex (Table 1).

As shown in Figure 3, the $[HTaO(OH)(\eta^2\text{-}O_2)]$ molecule was calculated to have a doublet ground state without

Table 1: Observed argon matrix and calculated (B3LYP/6-311++G**/SDD) vibrational frequencies (cm^{-1}) for [HTaO(OH)(η^2-O_2)] (C).

Mode	[HTaO(OH)(η^2-O_2)]		[DTaO(OD)(η^2-O_2)]		[HTa^{18}O(^{18}OH)(η^2-$^{18}O_2$)]	
	obs	calcd[a]	obs	calcd	Obs	calcd
O–H stretch	3699.3	3910.4(250)	2729.5	2849.6(162)	3687.5	3897.3(242)
Ta–H stretch	1838.7	1925.8(135)	1318.7	1366.9(69)	1838.5	1925.8(135)
O–O stretch	1113.8	1190.0(25)	1114.5	1189.6(24)	1051.7	1121.9(23)
Ta=O stretch	981.8	976.4(139)	982.0	975.4(136)	930.8	925.6(128)
Ta–OH stretch	739.0	734.7(94)	707.6	692.0(132)	716.7	721.9(57)
Ta–H bend	689.2	699.9(29)	521.9	517.9(25)	677.2	686.7(44)
Ta–H bend	623.9	647.0(10)	–	476.1(7)	619.4	637.9(10)
Ta–OH bend	501.9	496.4(162)	–	379.8(68)	477.1	488.1(173)
Ta–OH bend	451.0	486.2(131)	–	366.3(75)	443.7	478.9(138)
Ta–O_2 stretch	440.5	468.2(38)	–	212.5(21)	439.8	447.8(20)

[a] The intensities are listed in parentheses in km mol^{-1}. Only the vibrations above 400 cm^{-1} are listed.

symmetry. The O_2 subunit was predicted to be side-on bonded to the tantalum metal center with two slightly inequivalent Ta–O bonds. The observed O–O stretching vibrational frequency as well as the predicted O–O bond length (1.326 Å) indicate that [HTaO(OH)(η^2-O_2)] is a superoxide complex.[23,24] Thus, the complex can be formally described as [{HTaO(OH)}$^+${O_2}$^-$] with tantalum in its highest +V oxidation state. The calculated vibrational frequencies and intensities for [HTaO(OH)(η^2-O_2)] as well as isotopically substituted [DTaO(OD)(η^2-O_2)] and [HTa^{18}O(^{18}OH)(η^2-$^{18}O_2$)] are also listed in Table 1, which provide strong support for the proposed identification of this complex. The observed Ta–H, Ta=O, and Ta-OH stretching vibrational frequencies of [HTaO(OH)(η^2-O_2)] are higher than the corresponding modes of [HTaO(OH)]. These observations suggest that the Ta=O, Ta-OH, and Ta–H bonds in [HTaO(OH)(η^2-O_2)] with tantalum in +V oxidation state are stronger than those in [HTaO(OH)] with tantalum in +IV oxidation state because of increased electrostatic interactions.

The present experiments clearly indicate that the [TaO_2-(η^2-H_2)$_2$] complex was formed by the reaction of ground state TaO_2 and dihydrogen [Eq. (1)]. The [TaO_2(η^2-H_2)$_2$] complex can further be transferred to the [HTaO(OH)] molecule by photoisomerization in combination with H_2 elimination under visible-light iradiation. In the experiments with the H_2/O_2/Ar mixtures, the [HTaO(OH)(η^2-O_2)] complex was also produced on annealing after TaO_4, implying that [HTaO(OH)(η^2-O_2)] was formed through the reaction between TaO_4 and H_2 [Eq. (2)].

$$TaO_2\ (^2A_1) + 2\,H_2\ (^1\Sigma_g^+) \rightarrow [TaO_2(\eta^2\text{-}H_2)_2]\ (^2A_1) \qquad \Delta E = -3.6\ \text{kcal mol}^{-1} \tag{1}$$

$$TaO_4\ (^2A'') + H_2\ (^1\Sigma_g^+) \rightarrow [HTaO(OH)(\eta^2\text{-}O_2)]\ (^2A) \qquad \Delta E = -46.7\ \text{kcal mol}^{-1} \tag{2}$$

The potential energy profile for Equation (2) calculated at the B3LYP level of theory is shown in Figure 4. The reaction proceeds with the initial formation of a [TaO_4(H_2)] complex without any barrier. Unlike most of previously characterized metal dihydrogen complexes,[2,21,22] in which H_2 binds side-on to the metal primarily through both donation of the bonding σ electrons to vacant metal d orbital and back-donation of metal d electrons to the antibonding orbital of H_2, the bonding interaction between TaO_4 and H_2 only involves σ donation as TaO_4 is a d^0 complex. From the [TaO_4(H_2)] complex, one H atom transfers from Ta to one oxygen atom of tantalum dioxide subunit to form [HTaO(OH)(η^2-O_2)] via a transition state. The energy barrier from [TaO_4(H_2)] to [HTaO(OH)(η^2-O_2)] was predicted to be only 6.5 kcal mol^{-1}. The transition state has a four-center structure. Similar transition-state structures with low energy barriers have been reported in many metathesis reactions.[25,26] The overall TaO_4 + H_2 → [HTaO(OH)(η^2-O_2)] reaction was predicted to be exothermic by 46.7 kcal mol^{-1} and proceeds via a transition state that lies 3.7 kcal mol^{-1} lower in energy than the TaO_4 + H_2 reactants. The exothermicity of the overall reaction and the negative energy barrier height as compared to the reactants imply that the formation of [HTaO(OH)(η^2-O_2)] from TaO_4 + H_2 is both thermodynamically and kinetically favorable, which is consistent with the experimental observations.

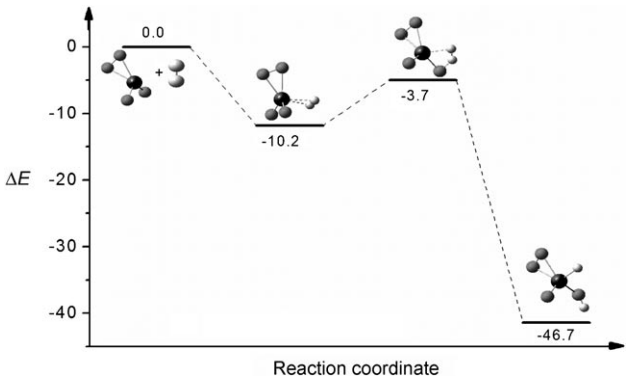

Figure 4. Potential-energy profile (ZPE corrected, in kcal mol^{-1}) for the TaO_4 + H_2 → [HTaO(OH)(η^2-O_2)] reaction calculated at the B3LYP/6-311++G**/SDD level of theory.

In contrast to TaO_4, which is able to cleave dihydrogen heterolytically and spontaneously at cryogenic temperatures, the cleavage of dihydrogen by TaO_2 requires activation energy. As mentioned above, the formation of [HTaO(OH)] from [TaO_2(η^2-H_2)$_2$] proceeds only under excitation with visible light. No products due to TaO + H_2 reaction were observed, indicating that the ground-state TaO molecule is unreactive toward H_2. These results indicate that the reactivity of tantalum oxides toward dihydrogen increases with the oxidation state, which follows the trend $Ta^{V}O_4 > Ta^{IV}O_2 > Ta^{II}O$. In the heterolytic cleavage of H_2 on TaO_x (x = 1, 2, 4), the reaction is concerted with a four-center cyclic transition state (Figure 4 and Figure S11 in the Supporting Informa-

tion). The activation barriers depend strongly on the strength of the Ta=O bond,[27] and follows the trend $TaO > TaO_2 > TaO_4$,[28] whereas the exothermicity of the reaction increases in the reverse order.

The present experiments clearly show that the neutral TaO_4 d^0 complex is able to cleave dihydrogen heterolytically and spontaneously at cryogenic temperatures in forming the $[HTaO(OH)(\eta^2\text{-}O_2)]$ complex, which involves both the hydridic (H^-) and the protic (H^+) functionalities. Thus, the $[HTaO(OH)(\eta^2\text{-}O_2)]$ complex may serve as a precursor to transfer hydrogen atoms to organic or other substrates. Theoretical calculations on prototype hydrogenation reaction of formaldehyde mediated by $[HTaO(OH)(\eta^2\text{-}O_2)]$ were performed, and the results are summarized in Figure S12 and Tables S4 and S7 in the Supporting Information. The calculated pathway of hydrogen transfer displays a double-well energetic profile involving two complex intermediates, which are linked via a transition state with a six-membered ring structure. A similar transition state has been reported for metal–ligand bifunctional catalyst mediated hydrogenation reactions.[29] The complete catalytic cycle $TaO_4 + H_2 + H_2CO \rightarrow TaO_4 + CH_3OH$ is predicted to be exothermic by 18.3 kcal mol^{-1} and proceeds via two transition states lying 3.7 and 23.9 kcal mol^{-1} lower in energy than the ground-state reactants: $TaO_4 + H_2 + H_2CO$. Therefore, the TaO_4 d^0 complex can serve as a model catalyst for hydrogenation reactions. The results presented herein may help in understanding the dihydrogen activation processes and catalytic mechanisms of hydrogenation reactions at metal centers.

Received: May 18, 2010
Published online: September 10, 2010

Keywords: density functional calculations · hydrogenation · matrix isolation · transition metals

[1] a) J. G. de Vries, C. J. Elsevier, *The Handbook of Homogeneous Hydrogenation*, Wiley-VCH, Weinheim, **2007**; b) S. Nishimura, *Handbook of Heterogeneous Catalytic Hydrogenation for Organic Synthesis* Wiley, Chichester, **2001**.
[2] G. J. Kubas, *Chem. Rev.* **2007**, *107*, 4152.
[3] G. J. Kubas, *Science* **2006**, *314*, 1096.
[4] R. D. Adams, B. Captain, *Angew. Chem.* **2008**, *120*, 258; *Angew. Chem. Int. Ed.* **2008**, *47*, 252.
[5] J. Spielmann, F. Buch, S. Harder, *Angew. Chem.* **2008**, *120*, 9576; *Angew. Chem. Int. Ed.* **2008**, *47*, 9434.
[6] T. Fujitani, I. Nakamura, T. Akita, M. Okumura, M. Haruta, *Angew. Chem.* **2009**, *121*, 9679; *Angew. Chem. Int. Ed.* **2009**, *48*, 9515.
[7] S. Fantasia, J. D. Egbert, V. Jurcik, C. S. J. Cazin, H. Jacobsen, L. Cavallo, D. M. Heinekey, S. P. Nolan, *Angew. Chem.* **2009**, *121*, 5284; *Angew. Chem. Int. Ed.* **2009**, *48*, 5182.
[8] X. F. Wang, L. Andrews, *Angew. Chem.* **2007**, *119*, 2656; *Angew. Chem. Int. Ed.* **2007**, *46*, 2602.
[9] a) F. H. Jardine, *Prog. Inorg. Chem.* **1981**, *28*, 63; b) R. H. Crabtree, *Acc. Chem. Res.* **1979**, *12*, 331.
[10] a) P. J. Brothers, *Prog. Inorg. Chem.* **1981**, *28*, 1; b) R. H. Morris, *Can. J. Chem.* **1996**, *74*, 1907; c) G. J. Kubas, *Adv. Inorg. Chem.* **2004**, *56*, 127; d) R. M. Bullock, *Angew. Chem.* **2007**, *119*, 7504; *Angew. Chem. Int. Ed.* **2007**, *46*, 7360; e) R. M. Bullock, *Chem. Eur. J.* **2004**, *10*, 2366.
[11] a) L. A. M. M. Barbosa, G. M. Zhidomirov, R. A. von Santen, *Catal. Lett.* **2001**, *77*, 55; b) K. Hermansson, M. Baudin, B. Ensing, M. Alfredsson, M. Wojcik, *J. Chem. Phys.* **1998**, *109*, 7515; c) L. J. Rodriguez, F. Ruette, M. Rosa-Brussin, *J. Mol. Catal.* **1990**, *62*, 199.
[12] D. K. Böhme, H. Schwarz, *Angew. Chem.* **2005**, *117*, 2388; *Angew. Chem. Int. Ed.* **2005**, *44*, 2336.
[13] a) D. Schroder, H. Schwarz, D. E. Clemmer, Y. M. Chen, P. B. Armentrout, V. I. Baranov, D. K. Bohme, *Int. J. Mass Spectrom. Ion Processes* **1997**, *161*, 175; b) M. F. Ryan, A. Fiedler, D. Schroder, H. Schwarz, *Organometallics* **1994**, *13*, 4072; c) M. F. Ryan, A. Fiedler, D. Schroder, H. Schwarz, *J. Am. Chem. Soc.* **1995**, *117*, 2033.
[14] H. Kang, J. L. Beauchamp, *J. Am. Chem. Soc.* **1986**, *108*, 5663.
[15] a) D. Y. Hwang, A. M. Mebel, *Chem. Phys. Lett.* **2001**, *341*, 393; b) D. Y. Hwang, A. M. Mebel, *J. Phys. Chem. A* **2002**, *106*, 520.
[16] a) G. J. Wang, M. F. Zhou, *Int. Rev. Phys. Chem.* **2008**, *27*, 1; b) M. F. Zhou, L. Andrews, C. W. Bauschlicher, Jr., *Chem. Rev.* **2001**, *101*, 1931.
[17] Y. Y. Zhao, Y. F. Huang, X. M. Zheng, M. F. Zhou, *J. Phys. Chem. A* **2010**, *114*, 5779.
[18] M. F. Zhou, L. Andrews, *J. Phys. Chem. A* **1998**, *102*, 8251.
[19] Y. Y. Zhao, X. M. Zheng, M. F. Zhou, *Chem. Phys.* **2008**, *351*, 13.
[20] The density functional theory calculations were performed using the hybrid B3LYP functional (A. D. Becke, *J. Chem. Phys.* **1993**, *98*, 5648; C. Lee, W. Yang, R. G. Parr, *Phys. Rev. B* **1988**, *37*, 785) with the 6-311++G** basis set for the H, C, and O atoms and the SDD pseudopotential and basis set for Ta (M. Dolg, H. Stoll, H. Preuss, *J. Chem. Phys.* **1989**, *90*, 1730; D. Andrae, U. Haussermann, M. Dolg, H. Stoll, H. Preuss, *Theor. Chim. Acta.* **1990**, *77*, 123). The geometries were fully optimized, and the harmonic vibrational frequencies were calculated with analytic second derivatives. The zero-point energies (ZPE) were derived. Transition-state optimizations were performed with the synchronous transit-guided quasi-Newton (STQN) method and were verified through intrinsic reaction coordinate (IRC) calculations. The single-point energies of the structures optimized at the B3LYP/6-311++G**/SDD level were calculated using a more larger basis set: aug-cc-pvtz for H, C, and O, aug-cc-pvtz-PP for Ta (D. Figgen, K. A. Peterson, M. Dolg, H. Stoll, *J. Chem. Phys.* **2009**, *130*, 164108). Further refinement of geometries and energetics was performed using the newly developed and well validated B2PLYP method (S. Grimme, *J. Chem. Phys.* **2006**, *124*, 034108), whereby the geometries were firstly optimized at the B2PLYP/6-311++G**/SDD level of theory and then by single-point energy calculations with the larger basis set. The results indicate that the B3LYP and B2PLYP methods agree well with each other (see the Supporting Information). Thus, the results reported in the text are given by the B3LYP method. All these calculations were performed by using the Gaussian 09 program (M. J. Frisch, et al. Gaussian 09, revision A02; Gaussian, Inc.: Pittsburgh, PA, **2009**).
[21] a) G. J. Kubas, R. B. Ryan, B. L. Swanson, P. J. Vergamini, H. J. Wasserman, *J. Am. Chem. Soc.* **1984**, *106*, 451; b) R. H. Crabtree, *Angew. Chem.* **1993**, *105*, 828; *Angew. Chem. Int. Ed. Engl.* **1993**, *32*, 789; c) F. Maseras, A. Lledos, *Chem. Rev.* **2000**, *100*, 601.
[22] a) M. F. Zhou, L. N. Zhang, L. M. Shao, W. N. Wang, K. N. Fan, Q. Z. Qin, *J. Phys. Chem. A* **2001**, *105*, 10747; b) H. S. Plitt, M. R. Bär, R. Ahlrichs, H. Schnöckel, *Angew. Chem.* **1991**, *103*, 848; *Angew. Chem. Int. Ed. Engl.* **1991**, *30*, 832.
[23] Y. Gong, M. F. Zhou, L. Andrews, *Chem. Rev.* **2009**, *109*, 6765.
[24] C. J. Cramer, W. B. Tolman, K. H. Theopold, A. L. Rheingold, *Proc. Natl. Acad. Sci. USA* **2003**, *100*, 3635.
[25] a) J. C. Weisshaar, *Acc. Chem. Res.* **1993**, *26*, 213; b) J. J. Carroll, K. L. Haug, J. C. Weisshaar, M. R. A. Blomberg, P. E. M. Siegbahn, M. Svensson, *J. Phys. Chem.* **1995**, *99*, 13955.

[26] a) S. Q. Niu, M. B. Hall, *Chem. Rev.* **2000**, *100*, 353; b) T. Ziegler, E. Folga, *J. Am. Chem. Soc.* **1993**, *115*, 636; c) L. Maron, O. Eisenstein, *J. Am. Chem. Soc.* **2001**, *123*, 1036.

[27] The Ta=O bond length was calculated to be 1.715, 1.749, and 1.761 Å for TaO ($^2\Delta$), TaO_2 ($^2A_1$), and TaO_4 ($^2A''$), respectively, at the B3LYP/6-311++G**/SDD level.

[28] The activation barrier for the $TaO(^2\Delta) + H_2 \rightarrow [HTaOH]$ ($^2A''$) was previously calculated to be 38.5 kcal mol^{-1} at the B3LYP/6–311++G**/Lanl2dz level (M. F. Zhou, L. N. Zhang, J. Dong, Q. Z. Qin, *J. Am. Chem. Soc.* **2001**, *123*, 135). The activation barrier for the TaO_2 ($^2A_1$) + $2H_2 \rightarrow [HTaO(OH)(\eta^2\text{-}H_2)]$ reaction was predicted to be 9.0 kcal mol^{-1} at the B3LYP/6-311++G**/SDD level.

[29] M. Yamakawa, H. Ito, R. Noyori, *J. Am. Chem. Soc.* **2000**, *122*, 1466.

